

A Hierarchical Modulation Enabled SNR Allocable Delta-Sigma Digital Mobile Fronthaul System

Yang Zou, Linsheng Zhong, Shenmao Zhang, *Member, IEEE*, Xiaoxiao Dai[✉], Jing Zhang[✉], Mengfan Cheng[✉], *Senior Member, IEEE*, Lei Deng[✉], *Senior Member, IEEE*, Songnian Fu[✉], *Senior Member, IEEE*, Qi Yang[✉], *Senior Member, IEEE*, and Deming Liu

Abstract—Internet of everything is being build up rapidly, which causes much higher requirements towards the flexibility of communication resources, especially the adaptivity of the fronthaul to various transmission distances and capacities. In this paper, we proposed a low-cost and spectrum efficient 5G fronthaul broadband connection solution that combines hierarchical modulation technology and delta-sigma modulation. The proposed scheme can double the number of accesses without occupying extra wavelengths. Moreover, such architecture can flexibly allocate the SNR of a group of remote radio units for different user requirement of transmission rate and reaches. Simulation results show that the proposed scheme can increase the access distance of the fronthaul network by 23% and the capacity by 16.7%. The feasibility of the solution is verified through a proof-of-concept experiment. After 20 km transmission, the OFDM-64QAM and -256QAM signal with a center frequency of 3.5 GHz and a bandwidth of 500 MHz can meet the EVM requirements of 8% and 3.5%, respectively. And when the R_{LM} of the hierarchical PAM4 signal is 0.6, the ROP required by the most-significant bit branch can be reduced by \sim 1.5 dB.

Index Terms—Flexible fronthaul network, hierarchical modulation (HM), signal-to-noise ratio (SNR) allocation, delta-sigma modulation.

I. INTRODUCTION

MERGING broadband services such as 8K video, virtual reality and augmented reality are driving the explosive growth of mobile data traffic. Mobile fronthaul (MFH) plays an important role in massive machine type communication (mMTC), and it faces many challenges. Firstly, the demand of IP traffic and number of accessed users are consistently

Manuscript received October 27, 2021; revised November 24, 2021; accepted December 9, 2021. Date of publication December 14, 2021; date of current version December 22, 2021. This work was supported by the Science and Technology Planning Project of Shenzhen Municipality under Grant JCYJ20200109142010888. (*Corresponding author: Xiaoxiao Dai*.)

Yang Zou, Linsheng Zhong, Shenmao Zhang, Xiaoxiao Dai, Mengfan Cheng, Lei Deng, Qi Yang, and Deming Liu are with the School of Optical and Electronic Information, Huazhong University of Science and Technology, Wuhan 430074, China (e-mail: zouyang@hust.edu.cn; zhonglinsheng@hust.edu.cn; zhangshenmao@hust.edu.cn; daixx@hust.edu.cn; chengmf@mail.hust.edu.cn; denglei_hust@mail.hust.edu.cn; yangqi@hust.edu.cn; dmliu@hust.edu.cn).

Jing Zhang is with the School of Optoelectronic Science and Engineering, University of Electronic Science and Technology of China, Chengdu 611731, China (e-mail: zhangjing1983@uestc.edu.cn).

Songnian Fu is with the School of Information Engineering, Guangdong University of Technology, Guangzhou 510006, China (e-mail: songnianfu@hotmail.com).

Digital Object Identifier 10.1109/JPHOT.2021.3135148

increasing, but the resources of optical fibers and available number of wavelengths is still limited [1]–[3]. Secondly, because of the characteristics of 5G wide connections, various wireless connection protocols and application scenarios with changing throughputs need to be supported at the same time [4]. For example, the 802.11ac protocol requires the terminal devices to support up to 256 quadrature amplitude modulation (QAM) modulation format, while protocol 802.11n only requires 64QAM. Besides, the IP traffic distribution may vary due to many factors, such as location and tidal effect. To meet these requirements, some flexible modulation schemes have been investigated to adaptively distribute signal quality. They can mainly be divided into two categories, the time-domain hybrid (TDH) modulation and hierarchical modulation (HM). In [5], a TDH-QAM transmission scheme achieves “continuous” spectral efficiency. The transmission rate is varied from 576 Gb/s to 1.15 Tb/s, while the transmission distances change from 5540 km to 470 km. Another TDH pulse amplitude modulation (PAM) – orthogonal frequency division multiplexing (OFDM) system is reported that the data rate of multiple sub-carriers with a fixed baud rate can be flexibly changed from 40 Gb/s to 80 Gb/s using mixed on-off keying (OOK) and PAM4 signals [6]. The TDH scheme can offer some intermediate system performance [7], [8]. Similarly, HM adaptively adjusts the signal quality of the two links within a group according to the user demands. It has been reported to be applied in OFDM passive optical network (PON) with a 2.7 dB power margin improvement [9]. What's more, HM has also been proved with PAM4 format in PON downstream systems to increase network power budget by 3.5 dB [10].

Currently, there are two major forms of MFH: analog fronthaul and digital fronthaul. For analog fronthaul, although the adoption of HM with analog signal has higher spectral efficiency, the signals are more susceptible to distortions caused by e.g., optical modulation or transport than in the case of digitized waveform [11]. This will lead to higher requirements for signal-to-noise ratio (SNR) of analog-to-digital conversion devices when the power ratio is high [12]. For digital fronthaul, the Common Public Radio Interface (CPRI) can hardly support huge mobile data transmission because of its low spectral efficiency. As an alternative solution for CPRI [13]–[14], delta-sigma modulation can transform an analog signal into a 1-or 2-bit digital signal. Multiple this kind of quantized 1-bit signal can be organized to form high-order PAM signals and HM. Constructing

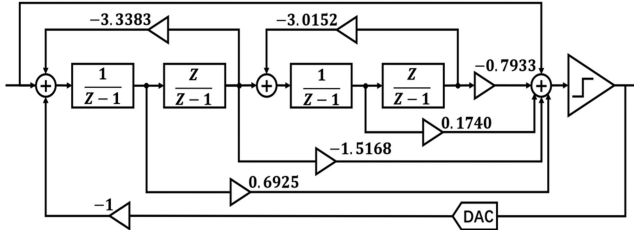


Fig. 1. A fourth-order delta-sigma modulator based on CRFF structure.

HM upon delta-sigma modulation instead of pure analog or digital waveforms only needs very simple logic circuits at the receiver side to complete hierarchical reception and filtering for signal retrieval, it avoids DSP and the use of digital-to-analog converter (DAC), which in turn avoids the increase in delay and power consumption caused by additional allocation processing in DSP and DAC [15]. Furthermore, this novel combination can be merged with multi-carrier aggregation technique, which can significantly enhance the wireless frequency flexibility.

In this paper, we proposed an approach combining the HM and delta-sigma modulation in MFH. The use of HM provides MFH a way to manage the downlink SNR through the optical layer, which enhances network flexibility. A PAM4 manner transmitter is used to combine the two 1-bit signal, so that quantity of the access users is doubled. Additionally, by modifying level mismatch separation ratio (R_{LM}), the received optical power (ROP) required by the two branches within a group can be reconfigured according to the signal quality demands in the receivers. Simulation results show that the proposed scheme can increase the access distance of the fronthaul network by 23% and the capacity by 16.7%. In the experiment, after 20 km transmission, the OFDM-64QAM and -256QAM signal with a center frequency of 3.5 GHz and a bandwidth of 500 MHz can meet the error vector magnitude (EVM) requirements of 8% and 3.5%, respectively. When the R_{LM} of the PAM4 signal is 0.6, the ROP required by the most-significant bit (MSB) branch can be reduced by ~ 1.5 dB.

II. OPERATION PRINCIPLES

A. Delta-Sigma Modulator

Delta-sigma modulation oversamples the analog signal to expand the area of quantization noise, and then pushes more quantization noise out of the signal band through noise shaping. The effect of noise shaping is determined by the structure and parameters of delta-sigma modulators. After 1-or 2-bit quantization, the analog signal is converted into OOK or PAM4 signal. At the receiver side, signal can be retrieved by using filters instead of DACs [13]. A fourth-order delta-sigma modulator based on cascade-of-resonators feedforward (CRFF) structure which is used in the following experiments is shown in Fig. 1. Its noise transfer function curve which is measured under the sampling rate of 10 GSa/s and the zero-poles plot are shown in Fig. 2. It can be seen that the specific delta-sigma modulator has an oversampling rate of 10 and a center frequency of 3.5 GHz.

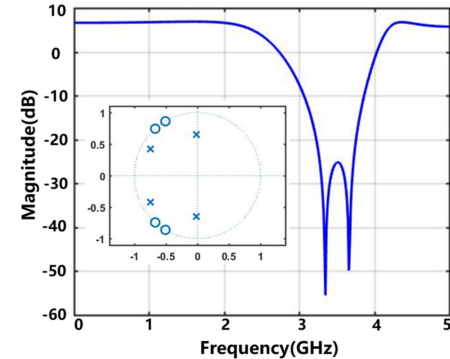


Fig. 2. NTF curve and the zero-poles plot.

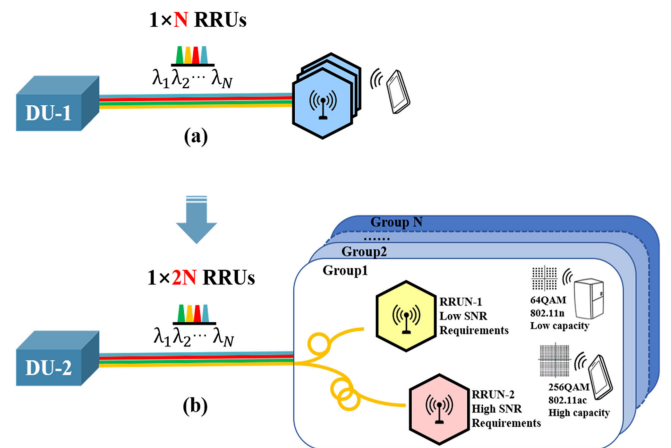


Fig. 3. (a) Schematic diagram of traditional delta-sigma MFH, (b) Schematic diagram of the proposed delta-sigma MFH using HM.

B. HM Based Delta-Sigma Modulation MFH

Our proposed scheme to double the number of accesses is shown in Fig. 3. In the traditional scheme shown in Fig. 3(a), N users can be accessed through the delta-sigma modulation based MFH. Each user corresponds to a 1-bit stream. In our scheme, two 1-bit streams are combined into a 2-bit PAM4 signal, which increases the number of accesses from N to $2N$. And the price paid for this is the sacrifice of SNR or power budget [16]. At the receiver side, after separating the MSB and less-significant bit (LSB) sequences, the modulated radio frequency (RF) analog signal can be retrieved. Fig. 3(b) shows the schematic diagram of a remote radio unit (RRU) group in our proposed HM MFH scheme. The RRUs are divided into several groups according to different SNR requirements caused by different transmission capacities or distances. Similar to [9], [10], a lower SNR required RRU is paired with another higher required one.

A hierarchical-PAM4 (H-PAM4) signal is the combination of two layers of OOK signals. By using Gray coding, the LSB/MSB sequence can be easily separated by high-speed logic circuits. We use R_{LM} metric, which is defined in IEEE 802.3bs [17], to quantify the degree of unequal separation level in the signal and

TABLE I
SIMULATION PARAMETER

Physical	Value	Unit
Net Rate	5.27 /6.15/7.03	Gbit/s
Wave Length	1550.5	nm
Emission Average Power	2e-3	W

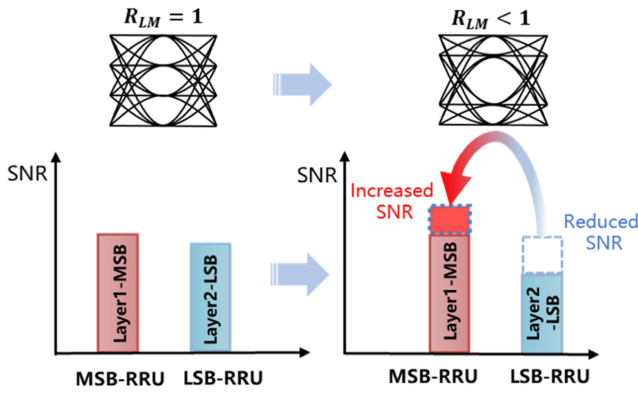


Fig. 4. Mechanism of SNR shift.

it is calculated with the following expression:

$$V_{mid} = \frac{V_0 + V_3}{2}, ES1 = \frac{V_1 - V_{mid}}{V_0 - V_{mid}}, ES2 = \frac{V_2 - V_{mid}}{V_3 - V_{mid}} \quad (1)$$

$$R_{LM} = \min \left\{ \begin{array}{l} (3 \times ES1), (3 \times ES2), \\ (2 - 3 \times ES1), (2 - 3 \times ES2) \end{array} \right\} \quad (2)$$

where V_0 to V_3 are the average values of the four H-PAM4 signal levels at the sampling point. R_{LM} will decrease when the center space between V_1 , V_2 is increased. Under this condition, the probability of misjudgment of the LSB level increases due to the decrease of the distance of the edge eye levels. On the contrary, the performance of MSB path will be improved. As shown in Fig. 4, by adjusting the R_{LM} value, the SNR provided to two links within a group can be redistributed. Therefore, the combination of delta-sigma modulation and HM can dynamically allocate the signal quality of the two branches to meet different users' demands.

III. NUMERICAL SIMULATION

To verify the capability of the proposed scheme, we first conducted a simulation on the proposed hierarchical delta-sigma modulation fronthaul scheme via commercial software VPI Transmissionmaker 9.9. The key simulation parameters are given in Table I. As shown in Fig. 5(a), the H-PAM4 signal is processed and analyzed in MATLAB after being transmitted by the IM/DD system. The launch power is fixed at 2e-3 W. A fourth-order low-pass Bessel filter with a 3 dB bandwidth of 16 GHz is used to limit the bandwidth to imitate the actual experimental situation and its frequency response is shown in Fig. 5(b). When the modulation formats of MSB and LSB are both 64QAM, the net rate is 900 (numbers of subcarriers)/1024

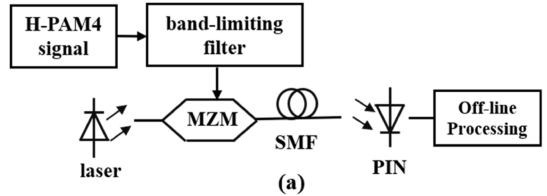


Fig. 5. (a) simulation setup, (b) frequency response of bandwidth limit filter.

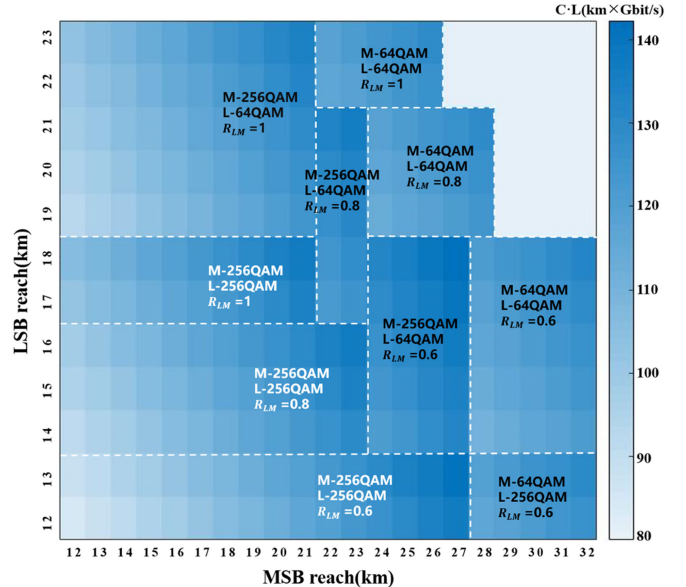


Fig. 6. The distance and capacity coverage of the proposed scheme.

(FFT size) \times 0.5 (bandwidth) \times 6 (bits per sample of 64 QAM) \times 2 (branch number) = 5.27 Gb/s. Similarly, the net rates of the other two modulation format combinations are 6.15 and 7.03 Gb/s, respectively.

Fig. 6 is a heat map of the relationship between the access distance and the modulation format. The abscissa and ordinate are the fiber extension distance of MSB and LSB respectively. Color depth of this figure represents the sum of distance capacity products of the MSB and LSB branches. And the entire 'map' is divided into blocks according to the combination of its lowest supported modulation format and the R_{LM} value. The available modulation formats are marked according to the 8% and 3.5% EVM requirements [13]. It can be seen that the coverage and capacity of the fronthaul network can be adjusted by changing R_{LM} . When the modulation formats of MSB and LSB are both 64QAM and $R_{LM} = 1$, the maximum reachable fiber length of

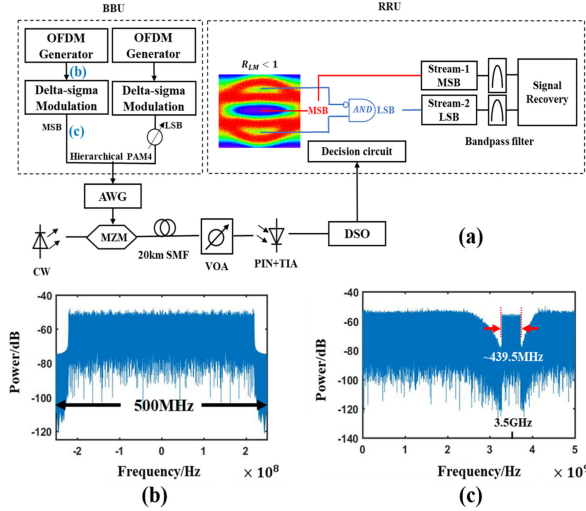


Fig. 7. (a) Experimental setup, (b) Spectrum of baseband OFDM signal, and (c) Spectrum of MSB signal.

MSB path is 26 km. When $R_{LM} = 0.6$, this coverage distance can be extended to 32 km, and the modulation format can support MSB and LSB corresponding to 64QAM and 256QAM. In this case, the access distance of a group is increased by 23%, and the capacity is increased by 16.7%. When both branches use 256QAM modulation format and R_{LM} is reduced from 1 to 0.6, the access distance of the group can be extended from 21 km to 27 km. In this case, the coverage distance of the network can be increased by 28.6%.

IV. EXPERIMENTAL SETUP

Fig. 7(a) shows the experimental setup for the proposed hierarchical digital MFH based on delta-sigma modulation. The OFDM-256QAM and -64QAM signals with sequence lengths of 384025 and 192025 are generated offline with a fast Fourier transform (FFT) size of 1024, in which 900 subcarriers are loaded with data. The sampling rate of OFDM signal is 500 MSa/s, resulting in 439.5 MHz effective bandwidth for OFDM signal. The spectrum is shown in Fig. 7(b). Subsequently, the analog signal is fed into the delta-sigma modulator, where the analog input is first oversampled to 10 GSa/s and then digitized into a 10 Gb/s OOK by 1-bit quantization, as is shown in Fig. 7(c). The other composing signal is also generated through the same process. At the same time, the attenuated amplitude of the LSB sequence is combined with the MSB sequence to form the final PAM4 signal after Gray coding.

By adjusting the threshold of the middle eye, a H-PAM4 signal with a constellation as given by Eq. (2) for various R_{LM} can be obtained. The resulting signal with a peak-to-peak value of 1 V is output by an arbitrary waveform generator (AWG, Keysight M8195A) working at 60 GSa/s. The H-PAM4 signal is used to modulate light from a 1550 nm continuous wave (CW) laser with a Mach-Zehnder modulator (MZM) and launch power is 10 dBm. After 20 km single mode fiber (SMF) transmission, a

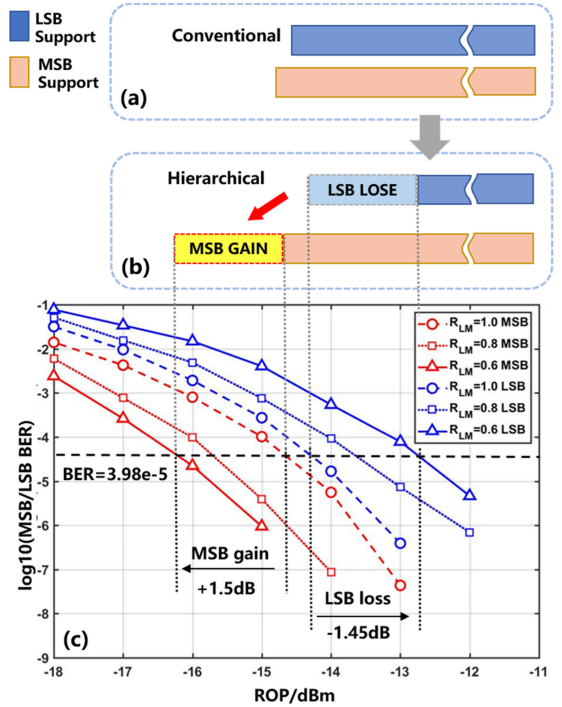


Fig. 8. (a) Energy distribution relationship of traditional PAM4 scheme, (b) Energy distribution relationship of H-PAM4 scheme, and (c) MSB/LSB BER performances with different R_{LM} .

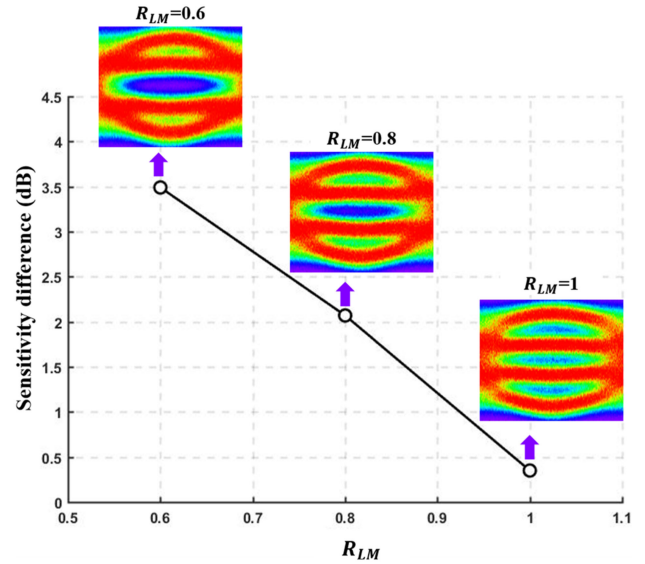


Fig. 9. Eye diagram and sensitivity differences between MSB and LSB with different R_{LM} .

variable optical attenuator (VOA) is cascaded for ROP adjustment, and a combination of PIN and trans-impedance amplifier (TIA) is used for optical-to-electrical (O/E) conversion. This signal is captured by a digital sampling oscilloscope (DSO, LeCroy SDA 830Zi-A) operating at 40 GS/s and stored for off-line processing. In the RRU, after retiming and synchronization, a T-spaced 5-tap feed forward equalizer (FFE) is adopted to

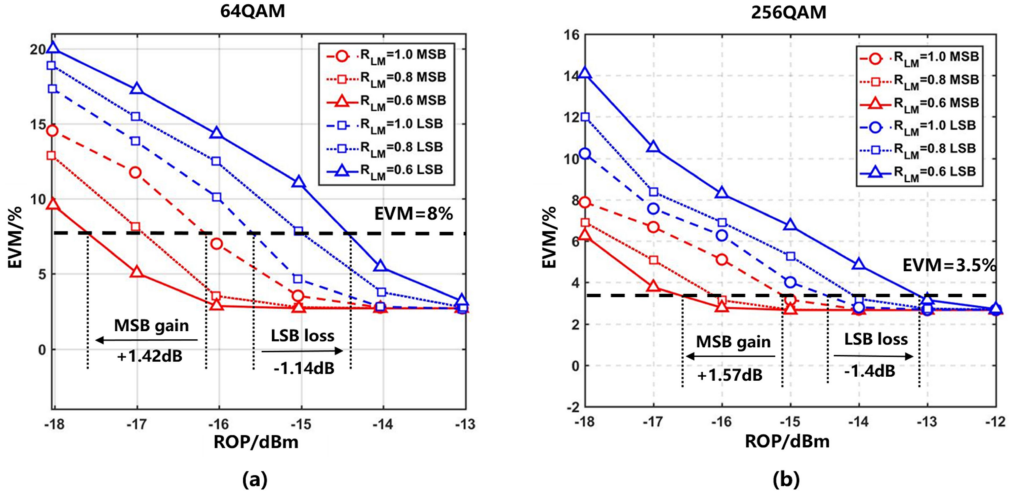


Fig. 10. (a) OFDM-64QAM EVM performances with different R_{LM} , (b) OFDM-256QAM EVM performances with different R_{LM} .

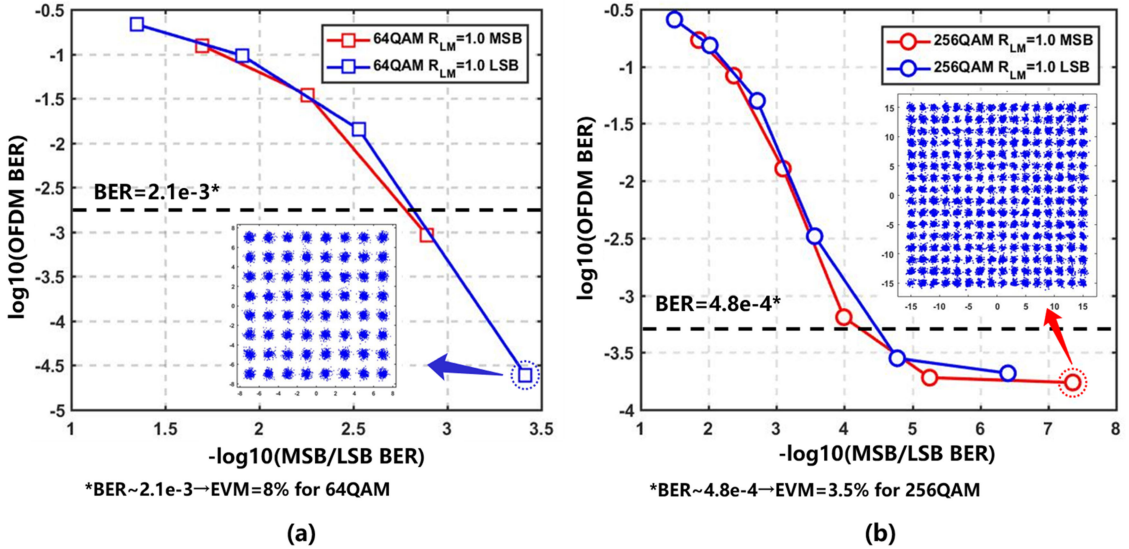


Fig. 11. (a) OFDM-64QAM BER vs. MSB/LSB BER, (b) OFDM-256QAM BER vs. MSB/LSB BER.

recover the received PAM4 signal. A bandpass filter is used to recover the original OFDM signal from the separated delta-sigma modulated bit sequences.

V. RESULTS AND DISCUSSIONS

As shown in Fig. 8(a), traditional PAM4 scheme will cause a mismatch between the demand and supply energy due to its fixed level interval. Instead, if the HM PAM4 scheme shown in Fig. 8(b) is used, the redundant power of the LSB sequence can be transferred to the MSB branch, so that enough SNR for both branches are guaranteed.

Fig. 8(c) depicts the BER results for 20 km transmission of 20 Gb/s H-PAM4 with three R_{LM} values. When $R_{LM} < 1$, reception of the MSB requires lower ROP, while the LSB requires higher. Specifically, when the BER threshold is set to 3.98e-5 and $R_{LM} = 1$, the difference of the received optical power required by the MSB and LSB is ~0.5 dB. Under the

same BER threshold, when R_{LM} is reduced to 0.6, the ROP required by the MSB RRU is reduced by ~1.5 dB compared to that when $R_{LM} = 1$, which can be used to support longer transmission distance. At the same time, the ROP required for LSB is also increased by ~1.45 dB. It should be noted that the EVM requirement of 256QAM is specified by 3GPP as 3.5%, which corresponds to the MSB/LSB BER level of 3.98e-5.

The sensitivity differences calculated with a BER threshold of 3.98e-5 between MSB and LSB under different R_{LM} values and the eye diagrams at ROP = -13 dBm are shown in Fig. 9. It can be seen that when the R_{LM} value is smaller, the eyes in the center of H-PAM4 will open wider. This means that the MSB sequence can provide a higher power margin. The sensitivity differences between MSB and LSB are 0.35 dB, 2.07 dB, and 3.49 dB when R_{LM} is 1, 0.8, and 0.6, respectively.

Fig. 10 illustrates the EVM performances versus ROP of the received OFDM signals carried by the MSB and LSB sequences. In this experiment, we set the minimum EVM requirement of

signal transmission for 256QAM and 64QAM to 3.5% and 8%, respectively. Under this setting, for the OFDM-256QAM signal, when R_{LM} is reduced from 1 to 0.6, the power budget of the MSB branch increases by ~ 1.57 dB, which also confirms the rationality of the BER threshold setting for the delta-sigma modulated sequences. The power budget reduction of OFDM-64QAM signal is ~ 1.42 dB.

In order to evaluate the relationship between the MSB/LSB damage and the user's BER, Fig. 11 illustrates the BER performances versus MSB/LSB BER of OFDM signal. R_{LM} will not affect the correspondence between the two variables, so only the case $R_{LM} = 1$ is shown here. It should be noted that the SNR provided by the OOK signal is limited to ~ 31 dB. For the 256QAM modulation format, although the BER of OOK signal is very low, the BER of OFDM signal is still on the order of 1e-4, as shown in Fig. 11(b). These errors are caused by the quantization noise in the signal band during delta-sigma modulation. Nevertheless, it is still lower than 4.8e-4 corresponding to the 3.5% EVM threshold of 3GPP. For the 64QAM modulation format, the SNR provided is sufficient. Moreover, only the BER of the OOK signal reaches ~ 3.84 e-4, and the OFDM signal will carry errors, as shown in Fig. 11(a). The corresponding constellation diagram is also given in the figure.

VI. CONCLUSION

We propose and experimentally verify a delta-sigma modulation and HM based MFH scheme. The proposed MFH scheme can double the number of accesses without occupying extra wavelengths and flexibly allocate the SNR of a group of RRUs. Our scheme can also be applied to higher-order modulation formats such as PAM6/8, which would further expand the number of supported RRU users. Furthermore, the proposed method can be merged with multi-carrier aggregation technique, which can significantly enhance the wireless frequency flexibility. Simulation results show that the proposed scheme can increase the access distance of the fronthaul network by 23% and the capacity by 16.7%. In the experiment, ROP enhancement is used to evaluate the capability of the proposed scheme to flexibly adjust a MFH system to different communication capacities and distances. Experimental results show that after 20 km transmission, when $R_{LM} = 0.6$, the ROP required by the 20 Gb/s H-PAM4 MSB OFDM-256QAM signal to reach 3.5% EVM can be reduced by ~ 1.5 dB. This means that the operator can select the corresponding R_{LM} configuration according to the distributed distance and capacity requirements of users, thereby increasing the overall aggregation capacity of the network without changing the links and devices.

REFERENCES

- [1] ITU-T G.694.2, *Spectral Grids for WDM Applications: CWDM Wave-Length Grid*, Accessed: Oct. 2020. [Online]. Available: <https://www.itu.int/itu-t/recommendations/rec.aspx?id=7057&lang=en>
- [2] ITU-T G.698.4, *Multichannel Bi-Directional DWDM Applications with Port Agnostic Single-Channel Optical Interfaces*, Accessed: Jan. 2018. [Online]. Available: <https://www.itu.int/itu-t/recommendations/rec.aspx?id=13519&lang=en>
- [3] IEEE 802.3cd, *Media Access Control Parameters for 50 Gb/s and Physical Layers and Management Parameters for 50 Gb/s, 100 Gb/s, and 200 Gb/s Operation*, Accessed: May 2018. [Online]. Available: https://standards.ieee.org/standard/802_3cd-2018.html
- [4] J. Yan, K. Shen, Y. Lin, J. Huang, C. Lin, and K. Feng, "Flexible capacity management for MMW-RoF mobile fronthaul with a polarization insensitive remote unit design," in *Proc. Opto-Electron. Commun. Conf.*, 2020, pp. 1–3.
- [5] Q. Zhuge, X. Xu, M. Morsy-Osman, M. Chagnon, M. Qiu, and D. V. Plant, "Time domain hybrid QAM based rate-adaptive optical transmissions using high speed DACs," in *Proc. Opt. Fiber Commun. Conf. Exhib.*, 2013, pp. 1–3.
- [6] T. Kodama, A. Maruta, N. Wada, and G. Cincotti, "Fixed-Rate-Breaking all-optical OFDM system using time-domain hybrid PAM with sparse subcarrier multiplexing and power-loading for optical short-reach transmission," in *Proc. Opt. Fiber Commun. Conf. Exhib.*, 2020, pp. 1–3.
- [7] Q. Zhuge, M. Morsy-Osman, X. Xu, M. Chagnon, M. Qiu, and D. V. Plant, "Spectral efficiency-adaptive optical transmission using time domain hybrid QAM for agile optical networks," *J. Lightw. Technol.*, vol. 31, no. 15, pp. 2621–2628, Aug. 2013.
- [8] R. Borkowski *et al.*, "World's first field trial of 100 Gbit/s flexible PON (FLCS-PON)," in *Proc. Eur. Conf. Opt. Commun.*, 2020, pp. 1–4.
- [9] P. Cao *et al.*, "Power margin improvement for OFDMA-PON using hierarchical modulation," *Opt. Exp.*, vol. 21, no. 7, pp. 8261–8268, Mar. 2013.
- [10] M. Dalla Santa, C. Antony, G. Talli, and P. D. Townsend, "Power budget improvement in passive optical networks using PAM4 hierarchical modulation," *IEEE Photon. Technol. Lett.*, vol. 29, no. 20, pp. 1747–1750, Sep. 2017.
- [11] A. Lorences-Riesgo, S. S. Pereira, D. C. Dinis, J. Vieira, A. S. R. Oliveira, and P. P. Monteiro, "Real-time FPGA-based delta-sigma-modulation transmission for 60 GHz radio-over-fiber fronthaul," in *Proc. Opt. Fiber Commun. Conf. Exhib.*, 2018, pp. 1–3.
- [12] K. Suzuoki, D. Hisano, S. Shiba, K. Maruta, and A. Maruta, "Nonlinear quantization for power-domain non-orthogonal multiple access passive optical network," *J. Lightw. Technol.*, vol. 39, no. 19, pp. 6142–6149, Oct. 2021.
- [13] J. Wang, Z. Jia, L. A. Campos, and C. Knittle, "Delta-Sigma modulation for next generation fronthaul interface," *J. Lightw. Technol.*, vol. 37, no. 12, pp. 2838–2850, Jun. 2019.
- [14] L. Zhong *et al.*, "Experimental demonstration of Delta-sigma modulation supported 65536-QAM OFDM transmission for Fronthaul/wifi applications," in *Proc. Eur. Conf. Opt. Commun.*, 2021, Paper Th2F.4.
- [15] H. Xin, H. He, K. Zhang, S. B. Hussain, and W. Hu, "Flexible baseband-unit aggregation enabled by reconfigurable Multi-IF over WDM fronthaul," *IEEE Photon. J.*, vol. 10, no. 1, Feb. 2018, Art. no. 7200210.
- [16] K. Zhong, X. Zhou, J. Huo, C. Yu, C. Lu, and A. P. T. Lau, "Digital signal processing for short-reach optical communications: A review of current technologies and future trends," *J. Lightw. Technol.*, vol. 36, no. 2, pp. 377–400, Jan. 2018.
- [17] IEEE 802.3bs, *Media Access Control Parameters, Physical Layers, and Management Parameters for 200 Gb/s and 400 Gb/s*, Accessed: Jun. 2017. [Online]. Available: https://standards.ieee.org/standard/802_3bs-2017.html